J Nanostruct 8(2): 107-118, Spring 2018

RESEARCH PAPER

Antimicrobial Activity and Photocatalytic Degradation Properties of Zinc Sulfide Nanoparticles Synthesized by Using Plant Extracts

Sathish kumar Mani [1], Saroja Manickam [2], Venkatachalam Muthusamy [2], Rajamanickam Thangaraj [1]*

[1] *Department of Electronics, Nehru arts and science college, Coimbatore, Tamilnadu, India*

[2] *Department of Electronics, Erode arts and science college, Erode, Tamilnadu, India*

ARTICLE INFO

Article History:
Received 14 February 2018
Accepted 08 March 2018
Published 01 April 2018

Keywords:
Photocatalytic degradation
Phyllanthusniruri
Syzygium aromaticum
Tridax procumbens
Zinc Sulfide

ABSTRACT

Biological synthesis of zinc sulfide (ZnS) nanoparticles (NPs) was prepared by a simple co-precipitation method using methanol plant extracts of Tridax procumbens, Phyllanthusniruri, and Syzygium aromaticum. The as-prepared ZnS NPs was examined by several physiochemical techniques such as X-Ray Powder Diffraction (XRD), Scanning Electron Microscopy (SEM), UV-Visible spectroscopy, Fourier Transform infrared spectroscopy analysis (FTIR). The disk diffusion method was used to screen the antimicrobial activity of Pure and Plant extracts doped ZnS NPs against different gram positive, gram-negative bacteria and fungus culture. From this investigation synthesized ZnS NPs have a potential antimicrobial agent where showed a hot zone of inhibition (ZOI) at different concentration against all tested microorganisms. Biosynthesized ZnS NPs Photocatalytic degradation also evaluated for Methylene Blue Dye (MBD) and Methyl Orange Dye (MOD) degradation in aqueous solution under UV Light irradiation. Due to the smaller particles size, narrowing optical band gap and antimicrobial properties of synthesised ZnS NPs were improve the photocatalytic activity. Here we first time reported Syzygium aromaticum methanol extracts ZnS NPs exhibited excellent efficiency in Methylene Blue Dye (MBD) and Methyl Orange Dye (MOD) degradation with comparing other ZnS NPs.

How to cite this article
Mani S. K, Manickam S, Muthusamy V, Thangaraj R. Antimicrobial Activity and Photocatalytic Degradation Properties of Zinc Sulfide Nanoparticles Synthesized by Using Plant Extracts. J Nanostruct, 2018; 8(2):107-118. DOI: 10.22052/JNS.2018.02.001

INTRODUCTION

The zinc sulfide (ZnS) is an essential semiconductor material in II-VI group with adirect and significant value of band gap energy (3.63–3.92 eV), with hexagonal wurtzite and cubic zinc blende crystal structure. The massive ionization transition and phase stable in normal atmosphere conditions is different properties of ZnS crystal [1-6]. There are various method has been utilized for the synthesis of ZnS NPs such as hydrothermal method, chemical vapor deposition, chemical bath deposition, chemical precipitation, chemical co-precipitation, γ irradiation route, sonochemical method, microwave irradiation, sol-gel technique, microemulsion method, thermal decomposition, solid-state reaction and solvothermal method [7-22]. From last two decades, ZnS semiconductor NPs are extensively investigated in various fields in electronics because of its excellent properties including optical, electrical, luminescence and photochemistry. The ZnS NPs have versatile potential applications in optoelectronics, ultraviolet light-emitting diodes, solar cells, field emitters, injection lasers, spintronics, infrared windows, sensors, photocatalysis, flat-panel displays, thin film electroluminescent devices,

* *Corresponding Author Email: mskeasc@gmail.com*

and antimicrobial activity [23-28]. The ZnS NPs have excellent photocatalytic degradation property especially inorganic pollutants dye such as Methylene Blue Dye (MBD), Rhodamine Blue Dye (RBD) and Methyl Orange Dye (MOD). The rapid generation of electron-hole pairs by photo-excitation and the highly negative reduction potentials of excited electronsandmetal-doped ZnS have been generated high electron-hole pair when treated under UV visible light,and it increases dye degradation propertydue to the influence of surface area and particle size of ZnS [29-40].

Recently, the green synthesis of ZnS NPs and the antibacterial ability was directly and strongly related to the concentration of ZnS NPs and different plant extract ZnS NPs using Corymbia citriodora, Fusarium oxysporum, Mushrooms, Elaeocarpus floribundas, Tridax procumbens, Phyllanthus Niruri, Syzygium Aromaticum extracts and plant family and medical usages also reported [41-48]. In this present work first time, we report biological synthesis of ZnS NPs using three different plants extracts of (Tridax procumbens, Phyllanthus Niruri, Syzygium Aromaticum), antimicrobial activity, Photocatalytic degradation of Methylene Blue Dye (MBD) and Methyl Orange Dye (MOD) degradation has been investigated.

MATERIALS AND METHODS

Preparation of plant extracts

The excellent growth, Matured Tridaxprocumbens and Phyllanthus niruri pants are collected from Nehru herbal garden Coimbatore, and Syzygiumaromaticum crude was purchased from Agriculture University at Coimbatore. All collected material washed with running tap water and Distilled water for remove dust, soils and treated shadow dry at 24 hours in room temperature then the dried materials were crushed to coarsely powdered by mixer and 250 g of coarse powder was subjected to successive extraction in 250 ml methanol solvent at 40^0 - 60^0 C by using soxhlet Apparatus [49-50] and collected three extracts were stored, used as capping agents and stabilizer for ZnS Fabrications.

Synthesis of ZnS nanoparticles

ZnS NPs were synthesized by using zinc sulfate ($ZnSo_4 7H_2O$), Thiourea (NH_2CSNH_2), Ammonia solution (NH_3) all materials good analytical grade (99% Purity) were purchased from Sigma-Aldrich, India. Typical synthesis process of Pure ZnS solution was obtained by mixing, 0.1 M of $ZnSo_4$, 0.1 M of Thiourea and 1% Ammonia solution 0.1 M of $ZnSo_4$ were dissolved in deionized water and the mixture was stirred for 30 min, then 1% ammonia solution was added drop by drop on this $ZnSo_4$ solution and the mixture was stirred continuously for 60 min while continuous stirring 0.1 M of Thiourea solution (which was kept continuous stirred for 30 min with deionized water and Thiourea) is added drop by drop on $ZnSo_4$ solution and mixture were kept 60 min stirringat room temperature.The resultant nanocolloid formation solution, itwas centrifugation at 2000 rpm for 20 Min then the solution was further treated air heated furnace at 60^0C for 5 hours then collected final crushed fine powder. For comparative evaluation of the three plant extract ZnS nanopowders was prepared the same experimental synthesis procedure presented above, but 20 ml of methanol extract was used as capping agent instead of ammonia complexing agent and the plant extract ZnS NPs was abbreviated as following namely Tridaxprocumbens plant extract synthesized ZnS - T:ZnS, Phyllanthusniruri plant extract synthesized ZnS - P:ZnS, Syzygium aromaticum crude extract synthesized ZnS – S:ZnS.

Characterization method

The pure and plant extracted ZnS NPs were successfully characterized by the following techniques, powder X-ray diffraction techniques used to determine the crystal structure of the NPs by (X'per PRO model) using CuKa radiation (λ = 1.54056 Å), at 40 keV in the 2Θ range of 10^0–80^0 with the step size of 0.1^0, The Hitachi S-4500 scanning electron microscope (SEM) help to found surface morphology and formation of nanoparticles with 5 kV acceleration voltage.The optical absorbance, electron absorbance spectra of the ZnS NPsis recordedby a Perkin Elmer UV/VIS/ NIR (λ=19) spectrophotometer withawavelengthrange of 300–900 nm at room temperature. JASCO FT/1 IR-6600 instrument was used to measure different bimolecular bondingfunction group with 400-4000 cm^{-1} spectral range, at spectral resolution record IR was 2 cm^{-1}.

Antimicrobial susceptibility test preparation

In vitro antimicrobial activity of pure and plant extract synthesized ZnS NPs were investigated by disc diffusion method against two gram

+ve and gram –ve bacterial cultures such as Staphylococcus aureus (S.aureus), Bacillus subtilis (B.subtilis) and Escherichia coli (E.coli), Pseudomonas aerugoinosa (P.aerugoinosa), also investigated against two fungus culture such as Candida albicans (C.albicans), and Aspergillus niger (A.niger) in a different concentration, all the culture are obtained from Microbial Type Culture Collection (MTCC) Institute of Microbial Technology,Chandigarh, India.One of the best antimicrobial susceptibility tests is disc diffusion method using Muller Hinton Agar (MHA) plates. MHA is obtained from Hi-Media Mumbai used to screening In vitro antimicrobial activity all the stock culture (staphylococcus aureus, Bacillus subtilis, Escherichia coli, Pseudomonas aerugoinosa, Candida albicans, Aspergillus niger) was maintained 4^0 C on slopes of nutrient agar, the loopful of cells process to treat transfer stock culture into test tube of Muller Hinton broth for bacteria that were incubated without agitation for 24 hrs at 37^0C and 25^0C respectively. The cultures were diluted with fresh Muller-Hinton broth to achieve optical densities corresponding to 2.0×10^6 colony forming units (CFU/ml) for bacteria, and fungus strains were inoculated separately in Sabourad's dextrose broth for 6 hours, and suspensions were approximately 10^5 CFU/ml. Before transfer the cultures the MHA plates are treated different process for purification, 15 ml pouring of molten media in to sterile plates, use to prepare MHA plates and allow 5 min for solidify then the minimum amount 0.1% of stock cultures inoculums were swapped in MHA plate surface and allowed 5 min to dry, The 60 mg/disc concentration disc is placed MHA plate surface each disc has 6mm width. The prepared pure and biosynthesized ZnS solution(for comparison evaluation) were loaded all disc surface with different concentration and allow 5 min to diffuse extracts,then the diffused MHA plates are kept Incubation at 37^0C for 24 hrs during the incubator zone of inhibition (ZOI) wasformed around the disc, transparent millimeter ruler use to determine ZOI [51, 52].

Photocatalytic experiment setup

The photocatalytic activity of ZnS,T:ZnS,P:ZnS,S:ZnS were evaluated by the Methylene Blue Dye (MBD) and Methyl Orange Dye (MOD) degradation under the 120 Whigh-pressure mercury lamp irradiation, the lamp was kept 10 cm distance between the liquid surface. Than 1.0 mg of photocatalyst was added in 100 ml (1×10^{-5} M) of MB and MO dye aqueous solution for comparative and mixture was stirred in dark for 30min to attain equilibrium condition on the catalyst solution and it was kept continuous stirring (180 min)throughout process of experiment, at regular time intervals (30 min), 3 ml of aqueous suspensions (MBD and MOD) was taken from the mixture and analyze concentration of degradation by usinga Perkin Elmer UV/VIS/ NIR (λ=19) spectrophotometer at wavelength of 623 nm for MBD and 461nmfor MOD respectively [53]. The photocatalytic degradation efficiency was calculated the following expression: Degradation efficiency (%) = $(C_0 – C) / C_0 \times 100$ % Here C is the concentration of suspensions MBD and MOD at each irradiated time interval, and C_0 is the initial concentration of MBD and MOD when equilibrium is achieved. For comparison evaluation, pure and synthesized ZnS NPs are used as a photocatalyst in the above-mentioned degradation process.

RESULT AND DISCUSSION

Crystalline Structure

Fig. 1 shows the X-ray diffraction pattern of ZnS, T:ZnS, P:ZnS and S:ZnS analyzed samples and all the diffraction peaks exhibits to corresponding synthesized ZnS NPs consistent of cubicphase structureswith lattice constant of a = b = 5.345 (Å)(JCPDS card no 80-0020), any other extra impurities diffraction peaks not detected from that so it is indicated well formation of ZnS NPs are obtained. Fig. 1(a) shows the diffraction peak pattern of pure ZnS in which 2Θ at 28.9^0, 48.1^0, 57.7^0 and 77.8^0 corresponding planes to the (111), (200), (311) and (331) reflection. The XRD spectrum of T:ZnS NPs shows the same major diffraction peaks of ZnS (hkl = 111) but the additional peaks of 2Θ at 33.5^0 and 69.8^0 to the corresponding plan (200) and (400) reflection, it was the evidence tridaxprocumbens plant extract were influenced crystalline growth of ZnS NPs as shown in Fig. 1(b).In addition Fig.1 (c-d) shows the six significant diffraction peak pattern of P:ZnS and S:ZnS in which 2Θ at 28.9^0,33.5^0,48.1^0,57.7^0,69.8^0 and 77.8^0 corresponding plane to the (111), (200),(220),(311), (400) and (331) reflection, in the presence XRD spectrum 2Θ at 69.8^0 of Syzygium aromatic extract was increase the peak broadening because of plant extract bonding with crystal contant of sulfur during annealing process,

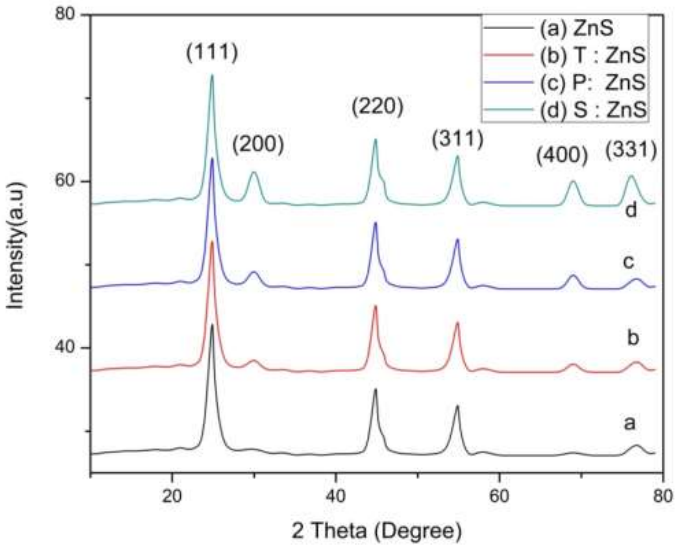

Fig. 1. XRD patterns of (a) ZnS, (b) T: ZnS, (c) P : ZnS, (d) S : ZnS

from this the plant extract are good bonding with ZnS NPs and influence to increase the crystallite size, the overall XRD spectrum intensity is increased with use of different plant extract . The average crystallite size (D) is estimated by Debye-Scherers formula based on the diffraction peak corresponding to the plane, In Table 1. The 2Θ, full-width half maximum (FWHM), D spacing,Crystalline size and band gap energy of synthesized ZnS NPs is given.

$$D = 0.9\lambda / \beta \cos \theta$$

Where D is crystallite size, 0,9 is the constant shape factor, λ=1.5405Å represents the wavelength of incident beam CuKa1, β is a full-width half maximum of the peak, Θ is diffraction angle in radian.

Morphological studies

The structural and morphological formation of pure and biosynthesized ZnS NPs are investigated by SEM image, and result are presented the NPs are spherical morphology with narrow particle size distribution, and the NPs formation was varied depends on the gapping (ZnS, P:ZnS, T:ZnS, S:ZnS) and complexing agent (NH_3) as shown in Fig. 2(a-d).

The S : ZnS nanoparticles are much smaller then ZnS, T: ZnS, and P: ZnS NPs, this indicated the plant extract might affect size of the ZnS NPs and size of NPs can be controlled by the plant extract, The diameter of the ZnS, T: ZnS, P : ZnS, and S : ZnS NPs are 143.5, 165.9,203.1 and 218.4 nm respectively. From the SEM image bio molecules of the plant extract were strong interaction with NPs surface, and quantities of the plant extract were leading the size reducing of spherical NPs [41-46].

Optical properties

The optical diffuse reflection absorbance spectroscopy of ZnS, T: ZnS, P : ZnS, and S: ZnS NPs are exhibited the maximum peak values, is shown in Fig. 3 from the result all the ZnS NPs have broad absorption peak at 323 nm for ZnS, 319 nm for P: ZnS, 313 nm for T: ZnS, 302 nm for S: ZnS respectively. The absorption peak of all plant extracts ZnS NPs maximum peak was blue shifted to compare pure ZnS. The band gap energy of Pure

Table 1. show the 2Θ, (hkl), FWHM, D spacing, crystallite size and Band gap energy of pure and synthesized ZnS NPs

Sample	2Θ (hkl)	FWHM (Radian)	D Spacing	Average Crystalline size (nm)	Band gap energy(eV)
ZnS	28.9 (111)	0.4795	3.13	17.87	3.85
T:ZnS	28.9 (111)	0.4799	3.15	17.84	3.90
P:ZnS	28.9 (111)	0.5056	3.28	16.94	3.97
S:ZnS	28.9 (111)	0.5102	3.45	16.71	4.12

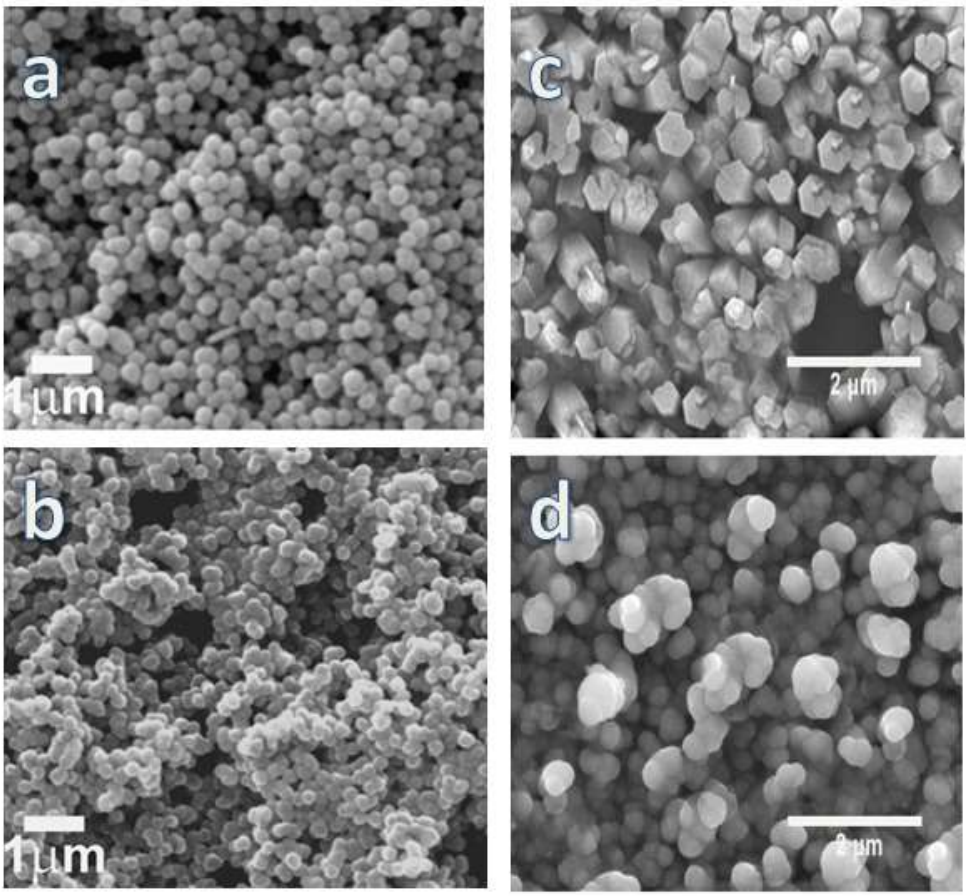

Fig. 2. SEM Image of (a) ZnS, (b) T: ZnS, (c) P : ZnS, (d) S : ZnS

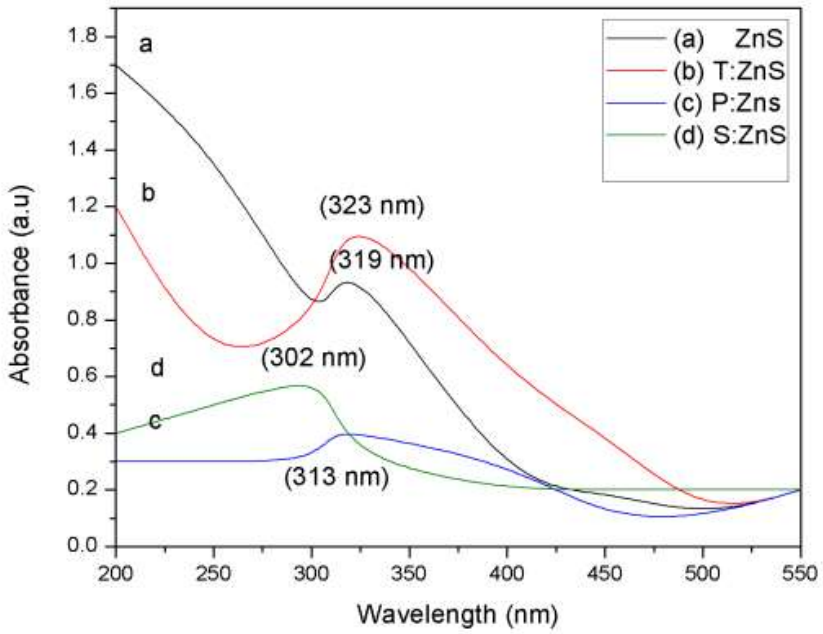

Fig. 3. Optical Absorbance of (a) ZnS, (b) T: ZnS, (c) P : ZnS, and (d) S : ZnS

and synthesized ZnS NPs was calculated using The Tauc's plots [54] for the samples and its relation between the absorption coefficient(α) and photon energy(hν).

$$\alpha h\upsilon=(h\upsilon-Eg)^{n}$$

Where, h isPlanck's constant, optical absorption co efficient is α, hν is photon energy, Eg is optical band gap, and n=1/2 is parameter associated with the electron transition for directly allotted, n=2 is indirectly allotted. The estimated values of the optical band gap of ZnS, T: ZnS, P: ZnS, and S: ZnS NPs is 3.85(eV), 3.90(eV), 3.97(eV), and 4.12(eV) respectively. From the result value, band gap was increased 3.85 (eV) to 4.12(eV), it was much higher than the bulk ZnS (3.7 eV) value is shown in Fig. 4 and table 1. The band gap was obtained from maximum absorption according to the quantum coefficient theory it was related to the electrons in the conductance band holes in the valence band are controlled by the potential barrier of the NPs surface due to presence of electrons and holes. The lowest optical transition from the valence band and conductance band is increase the band gap energy efficiently, from this result the plant extract was act as gapping agent and influence to increase the band gap energy and the particles size was reduced to compare pure ZnS.

Functional GroupAnalysis

The FTIR analysis for identifies the bimolecular absorption and different functional groups involved in the biosynthesis procedure, Fig. 5(a-d) shows the FTIR spectra for synthesized ZnS, T: ZnS, P: ZnS, and S: ZnS NPs. In Pure ZnS The broad absorbance peak 3110 cm^{-1} corresponds to hydroxyl,phenol(O-H) stretching, 1551 cm^{-1} corresponds to (C=O) stretching due to carboxylic, 1206 cm^{-1} absorbed (C-O) stretching correspond to epoxy, Amino acids, and 691 cm^{-1} is due to the presence of Zn-S water molecular stretching [55]. The plant extract ZnS FTIR was shown in Fig. 5(b-d)and all samples have thesame absorptionat (O-H, N-H),(C=O),(C-O) and Zn-S stretching peaks like pure ZnS. The T:ZnS have an additional peak at 2188 cm^{-1}due to (O=C=O) stretching, and broad peak 3110 cm^{-1} corresponds to (N-H) stretching in all plant extract ZnS. In P:ZnS have small peak at 2115 $cm^{-1}$and 2683 cm^{-1}due to alkenyl (C-H) stretching, The S:ZnS have very low peak at 1033 $cm^{-1}$and minimum absorption at 2194 cm^{-1}corresponding to the stretching of (C-C) due to alkenes and aromatics (C=C) from the various shifting of the peaks indicate different function group bioactive

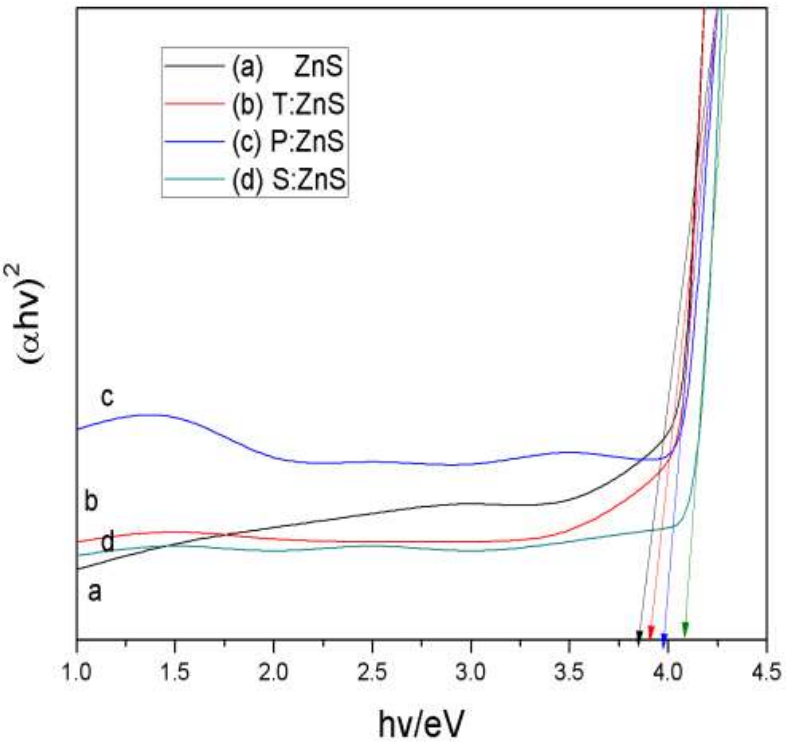

Fig. 4. Tauc's plot of (a) ZnS, (b) T: ZnS, (c) P : ZnS, and (d) S : ZnS

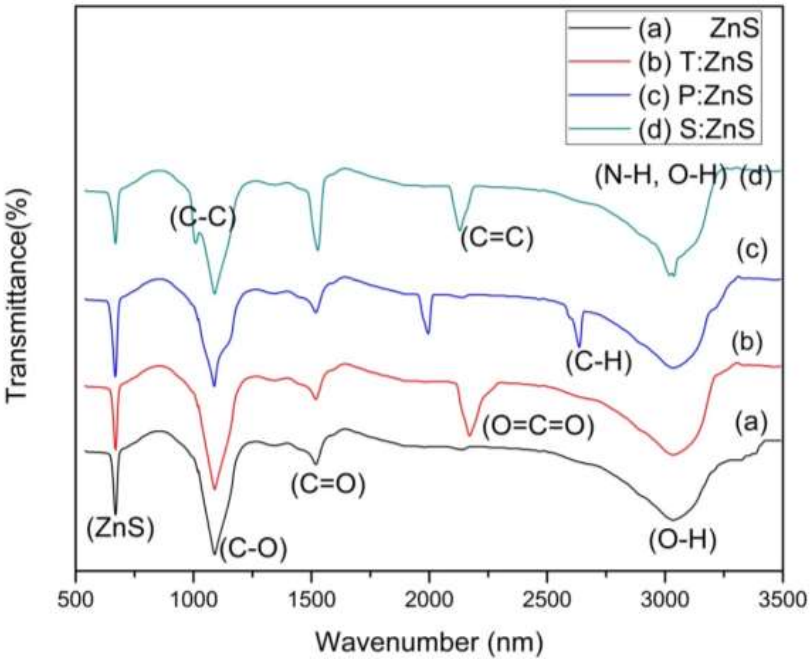

Fig. 5. FTIR spectra of (a) ZnS, (b) T: ZnS, (c) P : ZnS, and (d) S : ZnS

components(proteins, carbohydrate. Phenolic compounds, Amino acids) are commonly reduce and stabilize the ZnS NPs [46-48].

Antimicrobial Activity Analysis

The Antimicrobial activity of pure and biosynthesized ZnS NPs was evaluated by measuring zone of inhibition with various concentrations (40,50 and 60 (µg/mL)) against all tested microorganisms. The Antimicrobial activity of ZnS, T: ZnS, P : ZnS, and S : ZnS NPs were compared with two gram +ve and gram –ve bacterial cultures such as Staphylococcus aureus (S.aureus), Bacillus subtilis (B.subtilis) and Escherichia coli (E.coli), Pseudomonas aerugoinosa (P.aerugoinosa), also investigated against two fungus culture such as Candida albicans (C.albicans), and Aspergillus niger (A.niger) in a different concentration it was clearly shown in Table 2 and Fig. 6.

The pure ZnS NPs has highest inhibition zone was observed against E.coli (17± 0.1 mm) and C.albicans (17± 0.3 mm) followed by P.aerugoinosa (16± 0.1 mm), S.aureus (14± 0.2 mm), A. niger (14± 0.1 mm) and B.subtilis (13± 0.3 mm) at concentration of 60(µg/mL) from this resultconcentrationof ZnS NPs when extended the inhibition zone also increased.In T:ZnS NPs highest inhibition zone was formed against P.aerugoinosa(22± 0.1 mm) followed by E.coli (20± 0.1 mm),C.albicans(20± 0.2 mm), S.aureus(14± 0.2 mm), B.subtilis(18± 0.1 mm) and A. niger(15± 0.1 mm) at concentration of 60(µg/mL), from the starting concentration P.aerugoinosa has lead highest inhibition zone to compare other microorganisms. The P:ZnS NPs highest inhibition zone was observed against C.albicans (29± 0.1 mm) followed by E.coli (25± 0.1 mm), S.Aureus (23± 1.2 mm), B.subtilis (22± 0.3 mm), P.aerugoinosa (22± 0.2 mm) and A. niger (20± 0.3 mm) at a concentration of 60(µg/mL), from this result C.albicans inhibition zone was well formed from the beginning concentration. The S:ZnS NPs exhibits excellent antimicrobial activity against all tested microorganisms to compare other ZnS NPs, at concentration of 60(µg/mL) highest inhibition zone was observed against C.albicans (29± 0.3 mm) followed by E.coli (24± 0.1 mm),S.aureus (23± 1.2 mm), P.aerugoinosa (23± 0.1 mm) B.subtilis (22± 0.2 mm)and A. niger (21± 0.2 mm).From this results plant extract, ZnS NPs was high inhibition zone against gram +ve, gram –ve bacteria and fungus culture in various concentrations to compare pure ZnS NPs. From the comparison result maximum antimicrobial activity was observed by gram-negative bacterial than the gram-positive bacterialdue to their cell structure. The cell structure of both bacteria is different,

Table 2. show the Antimicrobial screening data of pure and synthesized ZnS NPs ZoI value* in (mm) concentration at (µg/mL)

Samples / Concentrations (µg/mL)	Gram (+ve) Inhibition zone (mm)						Gram (+ve) Inhibition zone (mm)						Fungi Inhibition zone (mm)					
	S.aureus			B.subtilis			E.coli			P.aerugoinosa			C.albicans			A. niger		
	40	50	**60**	40	50	**60**	40	50	**60**	40	50	**60**	40	50	**60**	40	50	**60**
ZnS	9	11	**14**	7	10	**13**	13	14	**17**	9	15	**16**	11	13	**17**	8	11	**14**
T:ZnS	15	18	**20**	10	13	**18**	16	17	**20**	16	19	**22**	14	18	**20**	11	13	**15**
P:ZnS	16	19	**23**	14	19	**22**	18	23	**25**	14	18	**22**	24	27	**29**	16	18	**20**
S:ZnS	14	20	**23**	16	20	**22**	15	19	**24**	16	19	**23**	18	25	**29**	18	20	**21**

* Average inhibition zone was varied from ± 0.1 to ±0.3 mm at all concentration

gram-positive bacteria have a single thick cell wall made up of peptidoglycan layer, and toxicity is very less due to the presence of thick layer. The gram-negative bacteria have double thin layered cell wall made up of lipopolysaccharide layer followed by peptidoglycan layer, this peptidoglycan layer is very thin to compare gram-positive layer and also it consist repeated unit of amino acids and carbohydrate, Thickness of the gram +vebacteria celllayer is 20-80 nm and gram –ve bacteria cell layer5-10 nm respectively. Here the ZnS, T: ZnS, P: ZnS, and S: ZnS NPs was discharged irons and react with amide phosphate, carboxyl in the protein of cell membrane and continuously disrupting the cell process and finally broke the cell wall and stop cell growth and formed inhibition zone around cell wallThe inhibition zone of C.albicans and A. niger fungus culture also investigated from the result C.albicans has formed maximum inhibition zone to compare A.niger because all ZnS NPs easily affect and penetrate the fungus cell membrane [46, 56]. The plant extracts ZnS NPs has a high antimicrobial activity to compare pure ZnS because plant extracts functional group biomolecules was controlled or killed the cell membrane of microorganisms. The small particle size and large surface area NPs exhibit high antimicrobial activity in which S:ZnS NPs have an excellent antimicrobial activity to compare other ZnS NPs.

Photocatalytic Activities

The photocatalytic activities of ZnS, T: ZnS, P: ZnS, and S: ZnS NPs sample were evaluated by degradation of Methylene Blue Dye (MBD) and Methyl Orange Dye (MOD) under visible light irradiation. Before adding the photocatalyst the MBD and MOD was treated photocatalytic degradation process to check the concentration efficiency under visible light irradiation from the result both dye only degrade 2% after 180 min of visible light irradiation, on the other side above the same process repeated MBD and MOD with 1.0 mg of ZnS, T: ZnS, P: ZnS, and S: ZnS NPs was a photocatalyst. During the irradiation electrons from the conduction band (CB) will excite to the valence band (vb) to increase electron-hole pair, a good photocatalyst act the adequate separation of electron and holes pair during the photogeneration, the holes of the valance band react with surface of the MBD and MOD bounded, react with water (H_2O) or Hydroxyl groups (OH^-) and generate hydroxyl radical (OH.) finally the conduction band(OH.) electrons reduce the MBD and MOD molecular oxygen to superoxide molecule to exert the degradation [42, 53]. The degradation of MBD and MOD concentration was higher in plant extract ZnS to compare pure ZnS.

Fig. 7 shows the degradation percentage of MBD at each 30 min Time interval using ZnS, T: ZnS, P: ZnS, and S: ZnS NPs, after 180 minute of irradiation, the photocatalytic degradation efficiency of MBD with ZnS, T: ZnS, P: ZnS, and S: ZnS NPs as photocatalyst (1.0 mg) is 55%, 68%, 73% and 81% respectively, the result plant extract using ZnS NPs have high photocatalytic efficiency to compare pure ZnS NPs, because the band gap energy of T: ZnS, P: ZnS, and S: ZnS NPs were increased, so it influence to increase photogeneration rate of electron/hole

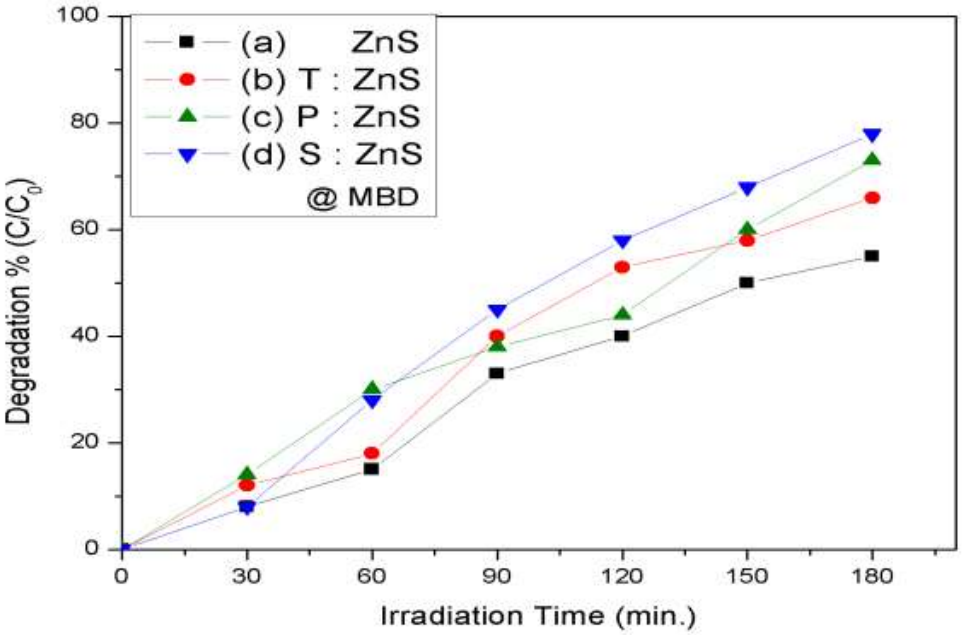

Fig. 7. Photocatalytic degradation efficiency of Methylene blue dye (MBD) using (a) ZnS, (b) T: ZnS, (c) P : ZnS, and (d) S : ZnS

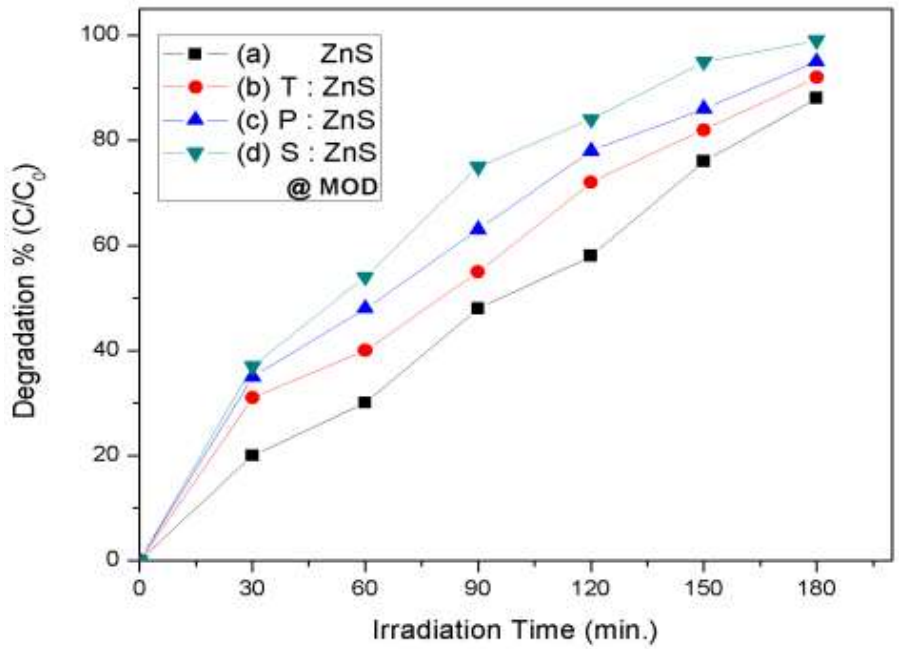

Fig. 8. Photocatalytic degradation efficiency of Methyl orange dye (MOD) using a) ZnS, (b) T: ZnS, (c) P : ZnS, and (d) S : ZnS

pair during light irradiation. Similarly, After 180 minute of irradiation the degradation efficiency of MOD using ZnS, T: ZnS, P: ZnS, and S: ZnS NPs as photocatalyst (1.0 mg)was investigated, from the Fig. 8 MOD degradation efficiency was found 90%, 92%, 95% and 99% respectively it was

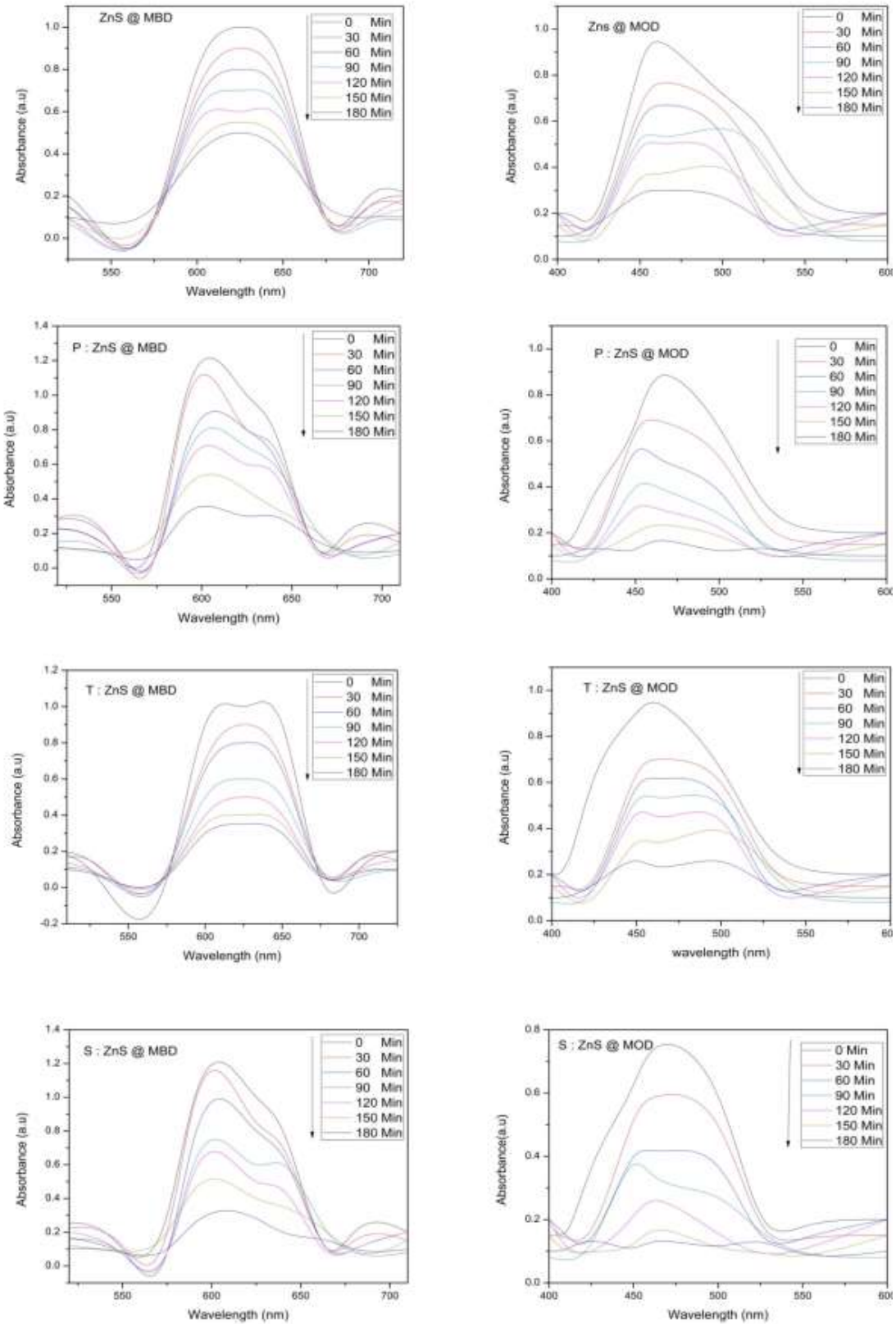

Fig. 9. UV Visible spectra of Photocatalytic degradation of Methylene blue dye (MBD) and Methyl orange dye (MOD) using ZnS, T: ZnS, P: ZnS, and S: ZnS NPs

evidence ZnS, T: ZnS, P: ZnS, and S: ZnS NPs is an excellent photocatalystwith MOD when compare MBD. Hence the percentage of photocatalyst was increased then the degradation efficiency also increases. The degradation spectra of MBD and MOD under the visible light irradiation was shown in Fig. 9 at constant time interval with using ZnS, T: ZnS, P: ZnS, and S: ZnS NPs separately. From the result degradation properties of the MBD and MOD was increased depends on the irradiation time and quantity of the photocatalyst.

CONCLUSION

In summary, the ZnS NPs was successfully synthesized by simple chemical co-precipitation method using plant extracts of Tridax procumbens, Phyllanthusniruri and Syzygium aromaticum. All the ZnS NPs were confirmed the cubic crystalline structure, and the average particle was 17 nm, to compare pure ZnS NPs the plant extract crystallite size was decrease and morphology of the ZnS NPs reveal thespherical shape of the particles and different diameter respectively. The optical band gap energy of pure and plant extract ZnS NPs was calculated from UV visible absorption spectra it is efficiently tuned from 3.83 eV to 4.10 eV efficiently, Tauc plots show this. The presence of different biomolecules bonding was confirmed by using FTIR spectra, which are involved the synthesis and stabilization of the ZnS NPs formation by using plant extracts. The antimicrobial activity of pure and plant extracts ZnS NPs wasinvestigated against gram positive, gram negative bacterial and fungus cultures, the excellent inhibition zone was formed against gram-negative bacterial and fungus, plant extract ZnS NPs has been reported high inhibition zone to compare pure ZnS NPs due to particle size and biomolecules present, the concentration of ZnS NPs was increased inhibition zone also increase. The synthesized ZnS NPs was foundan efficient photocatalyst for the degradation of Methylene blue dye (MBD) and Methyl orange dye (MOD). From the result Syzygium aromaticum extract ZnS NPs (1.0mg) exhibited excellent photocatalytic degradation of Methylene blue dye (MBD-81 %) and Methyl orange dye (MOD-99 %) under the visible light irradiation, organic pollutants dye degradation was increased depends on the photocatalyst percentage and irradiation time.

CONFLICT OF INTEREST

The authors declare that there are no conflicts of interest regarding the publication of this manuscript

REFERENCE

1. Wang L, Xudong X, Yuan X. Preparation and photoluminescent properties of doped nanoparticles of ZnS by solid-state reaction. J. Lumi., 2010; 130(1): 137–140.
2. Deng Z, Qi J, Zhang Y, Qingliang L, Huang Y. Growth mechanism and optical properties of ZnS nanotetrapods. J. Nanote., 2007; 18(1): 01-04.
3. Biswas S, Soumitra K. Fabrication of ZnS nanoparticles and nanorods with cubic and hexagonal crystal structures: a simple solvothermal approach. J. Nanote., 2008; 19(1): 01-11.
4. Yu SH, Yoshimura M. Shape and Phase Control of ZnS Nanocrystals: Template Fabrication of Wurtzite ZnS Single-Crystal Nano sheets and ZnO Flake-like Dendrites from a Lamellar Molecular Precursor ZnS (NH2 CH2 CH2 NH2)0.5. J. Adv. Mate., 2002; 14(4): 296-300.
5. Hengzhong Z, Banfield JF. Aggregation, coarsening, and phase transformation in ZnS nanoparticles studied by molecular dynamics simulations. J. Nano lett., 2004; 4(4): 713-718.
6. Moore D, Ronning C, Christopher M, Wang ZL. Wurtzite ZnS nanosaws produced by polar surfaces. J. Chem. Phys. Lett, 2004; 385(1): 08–11.
7. Masoud Salavati N, Mohammad Reza LE, Fatemeh D. Controllable synthesis of wurtzite ZnS nanorods through simple hydrothermal method in the presence of thioglycolic acid. J. Allo. Comp., 2009; 475: 782–788.
8. Masoud Salavati N, Fatemeh D, Mazaheri M. Synthesis and characterization of ZnS nanoclusters via hydrothermal processing from [bis(salicylidene)zinc(II)]. J. Allo. Comp., 2009; 470: 502–506.
9. Liu JZ, Yan PX, Yue GH. Synthesis of doped ZnS one-dimensional nanostructures via chemical vapor deposition. J. Mate. Lett., 2006; 60: 3471–3476.
10. Wei A, Liu J, Zhuang M. Preparation and characterization of ZnS thin films prepared by chemical bath deposition. Mate. Scie. Semi. Proc., 2013; 16: 1478–1484.
11. Wang X, Shi J, Feng Z, Li M, Li C. Visible emission characteristics from different defects of ZnS nanocrystals. Phys. Chem. Chem. Phys., 2011; 13(10): 4715–4723.
12. Sujata Devi L, K Nomita Devi K. Effect of Mn+2 doping on structural, morphological and optical properties of ZnS nanoparticles by chemical co-precipition method. J. Appl. Phys., 2014; 6(2): 06-14.
13. Zhang D, Limin Q, Cheng H, Jiming M. Preparation of ZnS Nanorods by a Liquid Crystal Template. J. Coll. Inte. Scie., 2002; 246: 413–416.
14. Hong Liao X, Jie Zhu J, Yuan Chen H. Microwave synthesis of nanocrystalline metal sulfides in formaldehyde solution. Mate. Scie. Engi., 2001; 85: 85–89.
15. Zhu J, Zhou M, Xu J, Liao X. Preparation of CdS and ZnS nanoparticles using microwave Irradiation. Mate. Lett., 2001; 47: 25–29.
16. Ying Lu H, Yuan Chu S, Seng Tan S. The Low-Temperature Synthesis and Optical Properties of Near-White Light Emission Nanophosphors Based on Manganese-Doped Zinc Sulfide. Jpn. J. Appl. Phys., 2005; 44(7): 5282–5288.
17. Kovtyukhov NI, Buzaneva EV, Waraksa CC, Mallouk TE. Ultrathin nanoparticle ZnS and ZnS: Mn films: surface sol–gel synthesis, morphology, photophysical properties. Mate. Scie. Engi., 2000;

69: 411–417.
18. Sobhani A, Masoud Salavati N, Sobhani M. Synthesis, characterization and optical properties of mercury sulfides and zinc sulfides using single-source precursor. Mate. Scie. Semi. Proc., 2013; 16: 410–417.
19. Masoud Salavati N, Davar F. Controllable synthesis of thioglycolic acid capped ZnS(Pn)0.5 nanotubes via simple aqueous solution route at low temperatures and conversion to wurtzite ZnS nanorods via thermal decompose of precursor. J. Allo. Comp., 2010; 494: 199–204.
20. Yu Zhou T, Quan Xin X. Room temperature solid-state reaction a convenient novel route to nanotubes of zinc sulfide. J. Nano Tech., 2004; 15: 534–536.
21. Wang L, Hong Y. A new preparation of zinc sulfide nanopartiles by solid state method by room temperature. Mate. Rese. Bull., 2000; 35: 695-701.
22. Zhao Q, Hou L, Huang R. Synthesis of ZnS nanorods by a surfactant-assisted soft chemistry method. Inor. Chem. Comm., 2003; 6: 971-973.
23. Kulkarni SK, Winkler U, Deshmukh N. Investigations on chemically capped CdS, ZnS and ZnCdS nanoparticles. Appl. Surf. Scie., 2001; 169: 438- 446.
24. Nizamoglu S, Ozel T, Sari E, Demir H. White Light Generation Using CdSe/ZnS Core–Shell Nanocrystals Hybridized with InGaN/GaN Light Emitting Diodes. Int. J. Nano tech., 2007; 18: 65-70.
25. Bouhafs D, Moussi A, Chikouche A, Ruiz J. Design and Simulation of Antireflection Coating Systems for Optoelectronic Devices: Application to Silicon Solar Cells. J. Sola. Ener. Mate. Sola. Cell., 1998; 52: 79-93.
26. Oladeji O, Chow L. Synthesis and Processing of CdS/ZnS Multilayer Films for Solar Cell Application. Thin Soli. Film., 2005; 474: 77-83.
27. Gang Chen Z, Cheng L, Yi Xu H, Zi Liu J. ZnS Branched Architectures as Optoelectronic Devices and Field Emitters. J. Adva. Mate., 2010; 22: 2376-2380.
28. Mirov SB, Fedorov W, Graham K, Moskalev I, Badikov V, Panyutin V. Erbium Fiber Laser–Pumped Continuous-Wave Microchip Cr2+:ZnS and Cr2+:ZnSe Lasers. J. Opti. Lett., 2002; 27: 909-911.
29. Sorokina T, Sorokin E, Mirov S, Fedorov V, Badikov V, Panyutin V. Broadly Tunable Compact Continuous-Wave Cr2+: ZnS. Lase. Opti. Lett., 2002; 27: 1040-1042.
30. Moore D, Wang Z. Growth of Anisotropic One-Dimensional ZnS Nanostructures. J. Mate. Chem., 2006; 16: 3898-3905.
31. Han J, Zhang W, Chen W, Thamizhmani L. Far- Infrared Characteristics of ZnS Nanoparticles Measured by Terahertz Time- Domain Spectroscopy. J. Phys. Chem., 2006; 110: 1989-1993.
32. Wu P, Miao L, Wang H, Shao X, Yan X. A Multidimensional Sensing Device for the Discrimination of Proteins Based on Manganese Doped ZnS Quantum Dots. Angew. Chem. Int. Edi., 2011; 50: 8118- 8121.
33. Tran PT, Goldman ER, Anderson GP. Use of Luminescent CdSe–ZnS Nanocrystal Bio conjugates in Quantum Dot-Based Nanosensors. J. Phys. Stat. Sol., 2002; 229(1): 427–432.
34. Zhang H, Chen X, Li Z, Kou J, Yu T, Zou Z. Preparation of Sensitized ZnS and its Photocatalytic Activity Under Visible Light irradiation. J. Phys. D: Appl. Phys., 2007; 40: 6846-6849.
35. Yen Lu M, Juann Chen L.Tunable electric and magnetic properties of CoxZn1−xS nanowires. J. Appl. Phys. Lett., 2008; 93: 01-05.
36. Rema Devi BS, Raveendran R, Vaidyan AV. Synthesis and Characterization of Mn2+-Doped ZnS Nanoparticles. Pram. J. Phys., 2007; 68: 679-687.
37. Manzoor K, Vadera SR, Kumar N. Multicolor Electroluminescent Devices Using Doped ZnS Nanocrystals. J. Appl. Phys. Lett., 2004; 84: 284-286.
38. Sathishkumar M, Saroja M. Antimicrobial activity of zinc sulphide nanoparticles and to study their characterization. Elix. Elec. Engg., 2016; 101:44118-44121.
39. Dong Seok Y, Hee Jae K. Local Structural Analysis for Mn-Doped ZnO Dilute Magnetic Semiconductors. Jpn. J. Appl. Phys., 2013; 52(10): 75-81.
40. Priyadharsini N, Elango M, Vairam S, Thamilselvan M. Effect of nickel substitution on structural, optical, magnetic properties and photocatalytic activity of ZnS nanoparticles. J. Mate. Scie. Semi. Proc., 2016; 49: 68–75.
41. Amir GR, Fatahian S, Kianpour N. Investigation of ZnS nanoparticle antibacterial effect. J. Curr. Nano Scie., 2014; 10: 796–800.
42. Jinfeng C, Binjie H, Jinhu Z. Optical and photocatalytic properties of Corymbia citriodora leaf extract synthesized ZnS Nanoparticles. Phys. E: Low dime. Syst. Nano Stru., 2016; 79:103-106.
43. Mirzadeh S, Darezereshki E, Bakhtiari F. Characterization of zinc sulfide (ZnS) nanoparticles Biosynthesized by Fusarium oxysporum. J. Mate. Scie. Semi. Proc., 2013;16 : 374–378.
44. Senapati US, Sarkar D. Structural, Optical, Thermal and Electrical properties of Fungus guided Biosynthesized Zinc Sulphide Nanoparticles. Rese. J. Chem. Scie., 2015; 5(1): 33-40.
45. Senapati US, Jha DK, Sarkar D. Structural, spectral and electrical properties of green synthesized ZnS nanoparticles using Elaeocarpus floribundus leaf extract. J. Mate. Scie. Mate. Elec., 2015; 8: 160-168.
46. Sathishkumar M, Saroja M. Biosynthesis and Characterization of Zinc Sulphide Nanoparticles using Leaf Extracts of Tridaxprocumbens. Orie. J. Chem., 2017; 33(2): 903-909.
47. Sathishkumar M, Saroja M. Characterization and antimicrobial activity of biosynthesised Zinc Sulphide Nanoparticles using phyllanthusniruri plant extract. Int. J. Chem. Scie., 2017; 5(2):123-131.
48. M Sathishkumar, M.Saroja. Green Synthesis, Characterization and Antimicrobial activity of ZnS using Syzygium aromaticum extract. Int. J. chemTech. Rese., 2017; 10(9): 443-449.
49. Subramanian R, Subbramaniyan P. Double bypasses soxhlet apparatus for extraction of piperine from Piper nigrum. Arab. J. Chem., 2016; 9: 537–540.
50. Krishan R, Kandasamy G. An evaluation of the efficacy of using selected solvents for the extraction of lipids from algal biomass by the soxhlet extraction method. Fuel., 2014; 116: 103–108.
51. John DT, James HJ. Antimicrobial Susceptibility testing: General Considerations. Manual of Clinical Microbiology, 7th edition, 2004.
52. Lalitha MK. Manual on Antimicrobial Susceptibility Testing, 2004.
53. Chen Y, Ma Q, Hanxiang J, Wang Y. Hydrothermal synthesis of ZnS microspheres with highly effective photocatalytic and antibacterial properties. J. Mate. Scie. Mate. Elec., 2016; 27(10):10237-10243.
54. Tauc J. Optical properties and electronic structure of amorphous Ge and Si. J. Mate. Rese. Bull. 1968; 3: 37–46.
55. Lellala K, Namratha K. Sol-gel assisted hydrothermal synthesis and characterization of hybrid ZnS-RGO nanocomposite for efficient photodegradation of dyes. J. Allo. Comp., 2016; 30:1-11
56. Brenda K, Wesley O, Nathan O. Synthesis, characterization and antimicrobial activity of ZnS nanoparticles. Ind. J. Nano., 2016; 4 (2): 1-6.